AD _____

OFFICE OF NAVAL RESEARCH

Contract N7onr-35801

T. O. I.

NR-041-032

Technical Report No. 81

STRESS AND VELOCITY FIELDS IN SOIL MECHANICS

by

R. T. Shield

GRADUATE DIVISION OF APPLIED MATHEMATICS

BROWN UNIVERSITY

PROVIDENCE, R. I.

December, 1952

A11-81/36

STRESS AND VELOCITY FIELDS IN SOIL MECHANICS[1]

by R. T. Shield

Brown University

Summary

Lines of discontinuity in the plastic stress field of a cohesive soil in a state of plane strain are discussed. The jump conditions on the stresses and the restrictions on the velocity field in the neighborhood of the line are obtained. The theory is applied to the problem of uniform pressure on one face of a wedge (or earth dam), and to the problem of a loaded trapezoid.

Finally, an analytic integration of the plane strain equations is carried out. Expressions are derived for the coordinates and curvatures of the failure lines and the velocity components at any point of a plastic stress field in terms of the boundary values.

[1]The results presented in this paper were obtained in the course of research sponsored by the Office of Naval Research under Contract N7onr-35801 with Brown University.

1. Introduction.

The solutions of many two-dimensional problems in soil mechanics are based upon the assumption that the soil is a plastic material in which slip or yielding occurs when the stresses satisfy the Coulomb formula [1][1]

$$f = \frac{1}{2}(\sigma_x+\sigma_y)\sin\varphi + \left\{\frac{1}{4}(\sigma_x-\sigma_y)^2 + \tau^2_{xy}\right\}^{1/2} - c\cos\varphi = 0, \qquad (1)$$

where c is the cohesion and φ is the angle of internal friction of the soil. Neglecting the weight of the soil, the stresses also satisfy the equations of equilibrium

$$\left.\begin{aligned} \frac{\partial\sigma_x}{\partial x} + \frac{\partial\tau_{xy}}{\partial y} &= 0, \\ \frac{\partial\tau_{xy}}{\partial x} + \frac{\partial\sigma_y}{\partial y} &= 0. \end{aligned}\right\} \qquad (2)$$

The two characteristic lines of the hyperbolic system of equations (1), (2) are inclined at an angle $\pi/4 + \varphi/2$ to the direction of the algebraically greater principal stress at any point. As in [2] the characteristic lines will be called the first and second failure lines, with the convention that the direction of the first failure line at a point is obtained from the direction of the algebraically greater principal stress by a clockwise rotation of amount $\pi/4 + \varphi/2$. The inclination of the first failure line to the x-axis will be denoted by θ.

Denoting the principal stresses by σ_1 and $\sigma_2(\sigma_1 < \sigma_2)$, it is convenient to introduce the quantity

$$p = \frac{(\sigma_2-\sigma_1)}{2\sin\varphi} \geq 0. \qquad (3)$$

---

[1] Numbers in square brackets refer to the bibliography at the end of the paper.

An arbitrary constant which has the dimensions of stress is sometimes introduced into the denominator of the expression for p in order to make p non-dimensional, but this practice will not be followed here. With the yield condition (1), it can be shown [3] that

$$\left.\begin{aligned} \sigma_x &= -p[1 + \sin\varphi \sin(2\theta + \varphi)] + c\cot\varphi, \\ \sigma_y &= -p[1 - \sin\varphi \sin(2\theta + \varphi)] + c\cot\varphi, \\ \tau_{xy} &= p \sin\varphi \cos(2\theta + \varphi), \end{aligned}\right\} \tag{4}$$

and the equations of equilibrium (2) can be replaced by the equations

$$\left.\begin{aligned} \tfrac{1}{2}\cot\varphi \log p + \theta &= \text{const. along a first failure line}, \\ \tfrac{1}{2}\cot\varphi \log p - \theta &= \text{const. along a second failure line}, \end{aligned}\right\} \tag{5}$$

These equations were obtained by Massau [4] for a cohesionless soil and by Kötter [5] for a cohesive soil.

Drucker and Prager [6] considered a proper generalization of the Coulomb hypothesis (1) and used the concept of plastic potential [7] to obtain a stress-strain law, assuming that the soil is a perfectly plastic body. In the case of plane strain, the stress-strain law corresponding to the yield function (1) is

$$\varepsilon_x = \lambda\frac{\partial f}{\partial \sigma_x}, \quad \varepsilon_y = \lambda\frac{\partial f}{\partial \sigma_y}, \quad \gamma_{xy} = \lambda\frac{\partial f}{\partial \tau_{xy}}, \tag{6}$$

where ε_x, ε_y, γ_{xy} are the plastic strain rates and λ is a non-negative factor of proportionality. With equations (4), the relations (6) can be written

$$\left.\begin{aligned} \varepsilon_x &= \frac{\lambda}{2}\{\sin\varphi - \sin(2\theta + \varphi)\}, \\ \varepsilon_y &= \frac{\lambda}{2}\{\sin\varphi + \sin(2\theta + \varphi)\}, \\ \gamma_{xy} &= \lambda \cos(2\theta + \varphi). \end{aligned}\right\} \tag{7}$$

It will be assumed that there is no deformation of the soil until plastic yielding occurs and therefore

$$\frac{\partial u}{\partial x} = \varepsilon_x, \qquad \frac{\partial v}{\partial y} = \varepsilon_y, \qquad \frac{\partial u}{\partial y} + \frac{\partial v}{\partial x} = \gamma_{xy},$$

where u,v are the components of velocity along the x,y-axes. The rate of dilation is found to be

$$\varepsilon_x + \varepsilon_y = \lambda \sin\varphi \geq 0, \tag{8}$$

so that plastic deformation must be accompanied by an increase in volume if $\varphi \neq 0$.

It was shown in [2] that the relations (7) imply that the rate of extension along the failure lines is zero. Also, the characteristic lines of the velocities coincide with the characteristic lines of the stresses and it is therefore convenient to refer the velocity equations to the characteristic lines. The orthogonal projections of the velocity vector on the directions of the first and second failure lines passing through the point are denoted by v_1 and v_2. The velocity projections v_1, v_2 are related to the cartesian components u,v of the velocity by the equations

$$\left.\begin{aligned} &v_1 = u\cos\theta + v\sin\theta, \quad v_2 = -u\sin(\theta+\varphi) + v\cos(\theta+\varphi), \\ &u = \{v_1\cos(\theta+\varphi) - v_2\sin\theta\}\sec\varphi, \quad v = \{v_1\sin(\theta+\varphi) + v_2\cos\theta\}\sec\varphi. \end{aligned}\right\} \tag{9}$$

The condition that the rate of extension along the failure lines is zero is expressed by the equations

$$\left.\begin{aligned} dv_1 - (v_1 \tan\varphi + v_2 \sec\varphi)d\theta = 0 \quad &\text{along a first failure line,} \\ dv_2 + (v_1 \sec\varphi + v_2 \tan\varphi)d\theta = 0 \quad &\text{along a second failure line,} \end{aligned}\right\} \quad (10)$$

and these equations, together with the velocity boundary conditions and the condition of non-negative dilatation, determine the velocity field when the failure lines are known.

Discontinuities in the velocity field were considered in [2] and it was shown that a line of discontinuity in the velocity field must be a failure line. The change in velocity across the line must be inclined at an angle φ to the line of discontinuity, so that a discontinuity in the tangential velocity is accompanied by a separation or a discontinuity in the normal velocity. In terms of the velocity projections v_1 and v_2, the requirement that the change in velocity is inclined at an angle φ to the line implies that either v_1 or v_2 is continuous across the line, according as the line is a second or first failure line respectively.

2. Discontinuities in the stresses.

In the theory of a Prandtl-Reuss material, for which $\varphi = 0$, the possibility of lines of discontinuity in the stress components is well known, and discontinuous stress fields have proved useful in many problems. Discontinuous stress fields are of value when limit analysis is used to obtain lower bounds for the collapse values of the surface tractions in a body or assemblage of bodies, even though the stress fields may be without obvious physical significance. It seems worthwhile,

therefore, to consider discontinuous plastic stress fields in a soil, not only from the viewpoint of obtaining real solutions but also with regard to future applications of limit analysis to soil mechanics. A discussion of stress discontinuities in a cohesionless heavy soil has been given previously by Massau [4]. The following discussion applies to a cohesive soil.

In Fig. 1, the line l-l represents an element of a line of stress discontinuity separating the plastic stress fields a and b. Subscripts a and b will be used to distinguish the values which a quantity assumes on the two sides of the line. The normal to the line is inclined at an angle Ω to the x-axis and, from equations (4), the normal and tangential tractions on such a line are

$$\left.\begin{aligned} N &= -p[1 + \sin\varphi \sin(2\theta-2\Omega+\varphi)] + c\cot\varphi, \\ T &= p \sin\varphi \cos(2\theta-2\Omega+\varphi). \end{aligned}\right\} \qquad (11)$$

The equilibrium of the small rectangular element shown in the figure requires that the normal and tangential components of stress N and T are continuous across the line, but the interior components N'_a, N'_b may be discontinuous. From equations (11), the equilibrium conditions are

$$\left.\begin{aligned} p_a[1+\sin\varphi \sin(2\theta_a-2\Omega+\varphi)] &= p_b[1+\sin\varphi \sin(2\theta_b-2\Omega+\varphi)], \\ p_a \cos(2\theta_a-2\Omega+\varphi) &= p_b \cos(2\theta_b-2\Omega+\varphi). \end{aligned}\right\} \qquad (12)$$

The elimination of p_a, p_b between these two equations gives, after some reduction,

$$\sin(\theta_a+\theta_b-2\Omega+\varphi) + \sin\varphi \cos(\theta_a-\theta_b) = 0, \qquad (13)$$

provided that $\sin(\theta_a-\theta_b) \neq 0$, that is, provided that the discontinuity is not of zero strength.

The condition(13) together with one of the conditions (12) correspond to the jump conditions established by Prager [8] for a Prandtl-Reuss material ($\varphi = 0$). For zero angle of friction, condition (13) becomes

$$\theta_a + \theta_b = 2\Omega \pm n\pi. \tag{14}$$

The Mohr's circles for the regions $\underline{a}$ and $\underline{b}$ are shown in Fig. 2, where p_a is taken greater than p_b for definiteness. The circles touch the yield locus

$$|\tau| = c - \sigma \tan \varphi,$$

since the regions are at the point of yielding. The stress point C has the coordinates $(N, -T)$ and the circles intersect at this point. The poles of the two circles are obtained by drawing a line through C parallel to the element $\dot{\ell} - \ell$ of the line of discontinuity. The points P_a, P_b where this line meets the circles are the poles of the circles. If A_a, B_a and A_b, B_b denote the points of contact of the circles $\underline{a}$ and $\underline{b}$ with the yield locus, then the lines P_aA_a, P_aB_a and P_bA_b, P_bB_b give the directions of the first and second failure lines in the regions $\underline{a}$ and $\underline{b}$ respectively. It can be seen from the diagram that the direction of the line of discontinuity lies in the acute angle formed by the failure lines in region $\underline{a}$ and in the obtuse angle formed by the failure lines in region $\underline{b}$.

It can easily be shown that a failure line cannot be a line of discontinuity in the stresses. Since a discontinuity in the velocity field can occur only across a failure line, it

follows that the velocity field must be continuous across a line of stress discontinuity. For a straight line of discontinuity, which may be taken to be parallel to the x-axis, the continuity of the velocity component u across the line implies that $\partial u/\partial x = \varepsilon_x$ is continuous across the line. This argument can be extended to show that ε_x is continuous across a curved line of stress discontinuity at any point P of the line, where the x-axis is taken parallel to the tangent to the line at P.

Considering first a Prandtl-Reuss material, equations (7) give

$$\varepsilon_x = -\frac{\lambda}{2} \sin 2\theta,$$

since φ is zero for this material. It follows that

$$\lambda_a \sin 2\theta_a = \lambda_b \sin 2\theta_b, \tag{15}$$

where λ_a, λ_b and θ_a, θ_b are the values assumed by λ and θ in the two stress fields at the point P. The jump condition (14) on θ_a, θ_b requires that

$$\theta_b = -\theta_a \pm n\pi. \tag{16}$$

Since the line is not a failure line, $\sin 2\theta_a \neq 0$, and the substitution of (16) in (15) gives

$$\lambda_a = -\lambda_b.$$

This equation implies that λ_a and λ_b are both zero at the point P because λ_a and λ_b are non-negative quantities. The plastic rate of strain is therefore zero at points on the line of discontinuity, and the line must be considered as a filament of non-plastic material. Elastic strains are neglected so that the

filament must be taken to bo inextensible but perfectly flexible. This conclusion has been reached previously [9,10] by assuming that the line of discontinuity is the limiting case of a narrow transition region in which the stress varies in a rapid but continuous manner.

In the same way, a line of stress discontinuity in a soil must be considered as an inextensible filament of non-plastic material. Apart from the algebra, the discussion is the same as the above discussion for a Prandtl-Reuss material, and it will not be given here.

3. Wedge under unilateral pressure. Stress solutions.

The problem of wedges with uniform pressure on one face will be considered in this section and in the following section. A continuous stress solution for obtuse angled wedges has been given by Prandtl [11] and the pattern of the failure lines is shown in Fig. 3a. The wedge ABE of angle β_0 ($\beta_0 \geq \pi/2$) is loaded by a uniform pressure P along AB, producing a plastic state of stress in the region ABEDC. The regions ABC, BDE are regions of constant stress and the region BCD is a zone of radial shear of angle $\beta_0 - \pi/2$. The pressure P required to produce plastic flow with this pattern of failure lines is given by

$$P = c \cot\varphi \left\{ \exp[(2\beta_0 - \pi) \tan \varphi] \tan^2\left(\frac{\pi}{4} + \frac{\varphi}{2}\right) - 1 \right\}. \quad (17)$$

The stress field of Fig. 3a is not applicable to acute angled wedges ($\beta_0 < \pi/2$) since the two constant stress regions ABC, BDE would overlap. However, the introduction of a line of stress discontinuity in the plastic stress region enables a stress solution to be found. Fig. 3b shows the wedge loaded along AB.

The constant stress regions ABC, BCD are separated by a line of stress discontinuity BC which is inclined to AB at an angle γ to be determined. AC and CD are first failure lines. The different values a quantity may assume in the regions ABC, BCD will be distinguished by the subscripts a and b respectively. Choosing the x,y-axes as shown in the figure, the inclination θ of the first failure lines assumes the values

$$\theta_a = 0, \qquad \theta_b = -(\pi/2 - \beta_0).$$

The substitution of these values into the jump condition (13), in which Ω is put equal to $\gamma - (\pi/4 - \varphi/2)$, gives the relation

$$\sin(\beta_0 - 2\gamma) + \sin\varphi \sin\beta_0 = 0.$$

This equation determines the angle γ and the relevant root of the equation is found to be

$$\gamma = \beta_0/2 + \mu/2, \tag{18}$$

where μ is given by

$$\sin\mu = \sin\varphi \sin\beta_0, \qquad 0 \leq \mu \leq \pi/2. \tag{19}$$

The value of p in the region BCD is determined by the condition of zero traction on BD and it has the value

$$p_b = \frac{c \cot\varphi}{(1-\sin\varphi)}.$$

The second equation of equations (12) then gives

$$p_a = \frac{c \cot\varphi}{(1-\sin\varphi)} \frac{\sin(\beta_0 - \mu)}{\sin(\beta_0+\mu)}.$$

With equations (11), the normal pressure on AB can now be found and a little rearrangement gives the value

$$P = c \cot \varphi \left\{ \tan^2\left(\frac{\pi}{4} + \frac{\varphi}{2} \right) \frac{\sin(\beta_0 - \mu)}{\sin(\beta_0 + \mu)} - 1 \right\} . \qquad (20)$$

When $\varphi = 0$ (Prandtl-Reuss material), μ is also zero and (20) takes the form

$$P = 2c(1 - \cos \beta_0),$$

agreeing with the value obtained by Prager [8]. For small values of β_0, expression (20) is approximately

$$P = c\beta_0^2 \cos \varphi ,$$

and it follows that for small values of β_0, the ratio P/c decreases as the angle of friction φ is increased. Fig. 4a shows the variation of P/c with the angle of the wedge for $\varphi = 0^\circ$, 20° and 40°. The limiting case $\varphi = 90^\circ$ is also shown in the diagram.

When $\beta_0 = \pi/2$, the expressions (17) and (20) have the common value $2c \tan (\pi/4 + \varphi/2)$, and the discontinuous solution is a continuation of the continuous solution. The full lines in Fig. 5b shows the variation in P/c with the wedge angle β_0 as furnished by the two solutions for angles of friction of 0°, 20° and 40°. The discontinuous solution also satisfies all the stress conditions when the angle of the wedge is greater than $\pi/2$, and the stress field, Fig. 3c, is an alternative solution to the continuous solution of Fig. 3a. However, it will be seen that a velocity field cannot be associated with the stress field of Fig. 3c, so that the discontinuous solution is not acceptable physically for wedge angles greater than a right angle. The pressure P as

finished by the discontinuous solution for obtuse angled wedges is again given by (20) and this value is lower than the value (17) obtained from the continuous solution. The broken lines in Fig. 4b give the values of P/c for varying $\beta_0 (\beta_0 \geq \pi/2)$ for angles of friction of 0°, 20° and 40°.

It should perhaps be pointed out that the line of discontinuity BC in Fig. 3c is not the line joining the point B in Fig. 3a to the point of intersection of the lines AC, ED except when the angle of friction is zero.

4. Wedge under unilateral pressure. Velocity solutions.

Without restricting the generality of the discussion, the boundary condition on the velocity field in the problem of the previous section may be taken to be that the normal velocity must have a given distribution on the loaded part AB of the wedge. The velocity in the plastic region has to be determined from this boundary condition and the boundary condition at the plastic rigid boundary. The given normal velocity along AB must be such that the resulting velocity field has non-negative dilatation everywhere and also, in the discontinuous stress solutions, the lines of stress discontinuity must behave as inextensible filaments.

Considering first the continuous stress field of Fig. 3a, the line ACDE, which is a first failure line, separates the region of plastic flow from the material which remains at rest. The velocity along ACDE must, therefore, be inclined at an angle φ to ACDE so that v_2 is zero along ACDE. Since the second failure lines are straight throughout the plastic region it follows that v_2 is zero everywhere. The value of v_1 along AB is known from the given normal velocity of AB and the fact that

v_2 is zero along AB. The variation of v_1 along the first failure lines is given by the first of equations (10) and knowing v_1 along AB it is a simple matter to obtain v_1 throughout the plastic region. The condition of non-negative dilatation will be satisfied provided that the given normal velocity of a point on AB is a non-decreasing function of the distance of the point from A.

Considering now the discontinuous stress field for the acute angled wedge, Fig. 3b, the velocity field must be such that the discontinuity line BC moves as an inextensible filament. Since the material below the plastic rigid boundary ACD remains at rest, this implies that the velocity component along BC is zero for points on BC. In determining the velocity field it is convenient to use oblique axes α,β having A as origin and directed along the first and second failure lines at A, Fig. 5. The normal velocity $f(\eta)$ is prescribed along AB, the line AB being given by $\alpha = \beta = \eta$.

The velocity field in the region ABC is determined in a very similar manner to that used by Lee [9] for the same problem in a Prandtl-Reuss material. It is unnecessary, therefore, to give the details. The value of v_1 in regions a and b of Fig. 5 is found to be

$$v_1(\beta) = 2 \cos\left(\frac{\pi}{4} - \frac{\varphi}{2}\right) f(\beta).$$

The velocity projection v_2 is zero in region a because of the boundary condition along AC, while in regions b and c it is given by

$$v_2(\alpha) = -2 \cos\left(\frac{\pi}{4} - \frac{\varphi}{2}\right) tf\left(\frac{\alpha-1}{t}\right),$$

where $t = \sin\psi \sec(\psi-\varphi)$, ψ is the angle BCF and where the length of AC is taken to be unity. For other points in the region ABC, v_1 and v_2 are given in the form of finite series. As the apex B is approached, the limiting expressions take the form

$$\left.\begin{aligned} v_1(\beta) &= 2\cos\left(\tfrac{\pi}{4}-\tfrac{\varphi}{2}\right) f(\beta) - t\left[2\cos\left(\tfrac{\pi}{4}-\tfrac{\varphi}{2}\right) f\left(\tfrac{\beta-1}{t}\right) - \right. \\ &\qquad \left. - t\left\{2\cos\left(\tfrac{\pi}{4}-\tfrac{\varphi}{2}\right) f\left(\frac{\frac{\beta-1}{t}-1}{t}\right) - \cdots\right\}\right]. \\ v_2(\alpha) &= -t\left[2\cos\left(\tfrac{\pi}{4}-\tfrac{\varphi}{2}\right) f\left(\tfrac{\alpha-1}{t}\right) - t\left\{2\cos\left(\tfrac{\pi}{4}-\tfrac{\varphi}{2}\right) f\left(\frac{\frac{\alpha-1}{t}-1}{t}\right) - \cdots\right\}\right]. \end{aligned}\right\} \quad (21)$$

The continued fractions which are the arguments of the function f in these expressions represent the coordinates of points on AB after successive reflections at BC and AB along lines parallel to the oblique axes at A.

It can readily be shown that the velocities v_1, v_2 approach limits at the vertex B. Also the limits are such that the velocity of the plastic field near B approaches the velocity of the non-plastic filament BC at B, this velocity being uniquely determined by the velocity condition on BC and the given normal velocity of AB at B.

The velocities of the points on the filament BC are now completely determined. The velocity of a point P in the region BCD is determined from the velocity of the filament BC and the boundary condition at the plastic rigid boundary CD. The velocity at P depends only upon the velocities of the points X, Y where the failure lines through P meet the line BC (see Fig. 5). v_1 is constant along PX, v_2 is constant along PY and

v_1 and v_2 are known at the points X,Y. If P lies in the region CDE then v_2 is zero.

The function $f(\eta)$ which specifies the distribution of normal velocity along AB can not be chosen in a completely arbitrary manner. Certain restrictions must be placed upon $f(\eta)$ in order that the dilatation be positive everywhere in the plastic region. The restrictions are most easily obtained in terms of the velocity $\chi(\ell)$ of the non-plastic filament at the point distance ℓ from C. $\chi(\ell)$ is continuous since the filament is non-plastic and also $\chi(0) = 0$ from the condition at C. Omitting the details of the analysis, it is found that the dilatation will be positive everywhere provided that $\chi'(\ell) \geq 0$ and $\chi'(\ell)$ is a non-decreasing function. These conditions imply that the rate of change of curvature of the filament increases towards the vertex. Thus the wedge behaves in a similar fashion to a beam which is bent by uniform loading.

The restrictions which have to be placed upon $f(\eta)$ are obtained by expressing $f(\eta)$ in terms of the restricted function $\chi(\ell)$.

In the discontinuous stress solution of Fig. 3c, the velocity conditions for the problem of the acute angled wedge apply in this case also. The plastic rigid boundary AC enforces $v_2 = 0$ along AC and it follows that $v_2 = 0$ throughout region ABC of Fig. 3c, since the failure lines are straight. The condition that the velocity component along BC is zero for points on BC then requires v_1 to be zero on BC and in consequence v_1 must be zero throughout the region ABC. Thus the velocity field obtained requires $f(\eta) = 0$ along AB and the solution does not

constitute plastic flow. The discontinuous stress solution for the obtuse angled wedge is therefore physically inadmissible.

5. Loaded trapezoid.

A further example of discontinuous stress fields is shown in Fig. 6a. The trapezoid ABCD is in a plastic state of stress due to the normal pressures P,Q on the parallel sides AB,CD, the sides AD,BC being free from applied traction. The lines AO, BO, CO, DO are lines of stress discontinuity separating the regions a, b, c, d of constant stress, where the angles marked γ, δ in the figure remain to be determined.

The stress boundary conditions require that

$$\theta_a = -(\tfrac{\pi}{4} + \tfrac{\varphi}{2}),$$

$$\theta_b = -(\tfrac{\pi}{4} + \tfrac{\varphi}{2}) + \chi,$$

$$\theta_c = -(\tfrac{\pi}{4} + \tfrac{\varphi}{2}),$$

where 2χ is the angle between the sides AD, BC and where the subscripts refer to the regions marked a, b, c in the figure. With these values of θ, the jump condition (13) at the discontinuity lines BO, CO show that

$$\cos(2\gamma + \chi) = \sin\varphi \cos\chi,$$
$$\cos(2\delta - \chi) = \sin\varphi \cos\chi,$$

and the relevant roots of these equations are

$$\gamma = \frac{\nu}{2} - \frac{\chi}{2}, \qquad \delta = \frac{\nu}{2} + \frac{\chi}{2},$$

where

$$\cos\nu = \sin\varphi \cos\chi, \qquad 0 \le \nu \le \frac{\pi}{2}.$$

The values of p in the regions $\underline{a}$ and $\underline{c}$ can be deduced from the known value of p in region $\underline{b}$ and the jump conditions (12) at the lines BO, CO. The pressures P, Q can then be obtained and it is found that

$$\left.\begin{aligned} P &= c \cot \varphi \left\{ \tan^2\left(\frac{\pi}{4} + \frac{\varphi}{2}\right) \frac{\sin(\nu+\chi)}{\sin(\nu-\chi)} - 1 \right\} , \\ Q &= c \cot \varphi \left\{ \tan^2\left(\frac{\pi}{4} + \frac{\varphi}{2}\right) \frac{\sin(\nu-\chi)}{\sin(\nu+\chi)} - 1 \right\} . \end{aligned}\right\} \qquad (22)$$

As the angle of friction φ tends to zero these expressions tend to the values

$$P_0 = 2c(1+\sin \chi), \qquad Q_0 = 2c(1-\sin \chi),$$

agreeing with the values obtained by Winzer and Carrier [12] for a Prandtl-Reuss material.

It can be shown that a velocity field can not be associated with the stress field of Fig. 6a. This follows in the same way in which it was shown that a velocity field could not be associated with the stress field of Fig. 3c. The stress field is therefore physically inadmissible.

If the sides AD, BC of the trapezoid are continued beyond the points D, C a truncated wedge is obtained. A solution corresponding to a uniform pressure on the top surface of the wedge has been given by Prandtl [9] and the stress field is outlined in Fig. 6b. The value of the normal pressure P' is in this case

$$P' = c \cot \varphi \left\{ \tan^2\left(\frac{\pi}{4} + \frac{\varphi}{2}\right) \exp(2\chi \tan \varphi) - 1 \right\} .$$

and this value is greater than the value P given by equation (22). A velocity field can be associated with the stress field

of Fig. 6b provided that the given normal velocity of the points on AB is constant or a monotonic function of the distance from A.

6. Integration of the plane strain equations.

In obtaining solutions to plasticity problems in soil mechanics the stress distribution can not always be built up from the simple failure patterns of the Rankine zones and the zone of radial shear. In complex problems involving fields of varying stress it is usual to obtain the stresses by approximate numerical methods [3]. In this section exact expressions will be derived for the coordinates and curvatures of the failure lines and the velocity components at any point of a stress field in terms of the boundary values. However, the expressions involve integrals which can be evaluated in finite form only when the boundary conditions are particularly simple. For this reason the analysis is of limited importance and, as in the theory of a Prandtl-Reuss material, will mainly be of value in checking the accuracy of the usual approximate methods.

In Fig. 7, the x, y-axes are taken at a point O along and normal to the direction of the first failure line at O. The first and second failure lines OA and OB will be called the α base-line and the β base-line respectively. The curvilinear coordinates of a point P are defined by the pair of quantities (α,β); where α is the value of θ at the point A where the second failure line through P meets the α base-line OA, and where β is the value of θ at the point B where the first failure line through P meets the β base-line OB. The correspondence between (α,β) and the coordinates (x,y) of P is

one to one except when one of the families of failure lines is straight. It follows from the definition that α and β are constant along the second and first failure lines respectively, and the base-lines are given by $\beta = 0$ and $\alpha = 0$.

With equations (5) it is not difficult to show that

$$\left.\begin{aligned} \theta &= \alpha + \beta , \\ \tfrac{1}{2} \cot \varphi \log p &= \beta - \alpha + \tfrac{1}{2} \cot \varphi \log p_0, \end{aligned}\right\} \qquad (23)$$

where θ and p are evaluated at the point P and p_0 is the value of p at the origin O. The first of equations (23) is a statement of what is usually known as Hencky's first theorem [13], which is expressed analytically by

$$\theta_P - \theta_B = \theta_A - \theta_0. \qquad (24)$$

The theorem was first stated by Massau [4] for the case of a cohesionless soil. Equation (23) can be re-arranged to give

$$\left.\begin{aligned} 2\alpha &= \tfrac{1}{2} \cot \varphi \log p_0 - (\tfrac{1}{2} \cot \varphi \log p - \theta), \\ 2\beta &= - \tfrac{1}{2} \cot \varphi \log p_0 + (\tfrac{1}{2} \cot \varphi \log p + \theta). \end{aligned}\right\} \qquad (25)$$

Coordinates $\bar{x},\bar{y}$ are introduced by means of the equations

$$\left.\begin{aligned} &\bar{x} = x \cos(\theta+\varphi) + y \sin(\theta+\varphi), \quad \bar{y} = -x \sin \theta + y \cos \theta, \\ &x = \{\bar{x} \cos \theta - \bar{y} \sin(\theta+\varphi)\} \sec \varphi, \quad y = \{\bar{x} \sin\theta + \bar{y} \cos(\theta+\varphi)\} \sec \varphi. \end{aligned}\right\} \qquad (26)$$

The geometrical significance of the coordinates $(\bar{x},\bar{y})$ is shown in Fig. 8; $\bar{x}$ and $\bar{y}$ are the distances of the origin O from

the tangents to the second and first failure lines at P. The coordinates $\bar{x},\bar{y}$ have been used in the theory of the Prandtl-Reuss material [14]. On a first failure line (on which $dy = \tan\varphi\, dx$) equations (26) give

$$d\bar{y} = -\sin\theta\, dx + \cos\theta\, dy - (x\cos\theta + y\sin\theta)\, d\theta$$
$$= -(\bar{x}\sec\varphi - \bar{y}\tan\varphi)\, d\theta,$$

and therefore

$$d\bar{y} + (\bar{x}\sec\varphi - \bar{y}\tan\varphi)d\theta = 0 \text{ along a first failure line.} \qquad (27)$$

Similarly,

$$d\bar{x} - (\bar{y}\sec\varphi - \bar{x}\tan\varphi)d\theta = 0 \text{ along a second failure line.} \qquad (28)$$

The radii of curvature R,S of the first and second failure lines at the point P are defined by

$$\frac{1}{R} = \frac{\partial\theta}{\partial s_1}, \qquad \frac{1}{S} = -\frac{\partial\theta}{\partial s_2}, \qquad (29)$$

where s_1 and s_2 are the arc-lengths along the first and second failure lines. Fig. 9 shows the intersection of two neighboring first failure lines with two neighboring second failure lines. The small angles $\theta_B - \theta_A$, $\theta_D - \theta_A$ will be denoted by $\Delta\theta_1, \Delta\theta_2$ respectively. In the figure, $\Delta\theta_1$ is positive while $\Delta\theta_2$ is negative. It follows from the definitions (29) that

$$R\Delta\theta_1 = \Delta s_1, \qquad S\Delta\theta_2 = -\Delta s_2 \qquad (30)$$

and therefore

$$\frac{\partial}{\partial s_2}(R\Delta\theta_1) = \frac{\partial}{\partial s_2}(\Delta s_1). \qquad (31)$$

From the geometry of Fig. 9 and equations (30),

$$DC = \Delta s_1 - \Delta\theta_1 \sec\varphi\, \Delta s_2 - \Delta\theta_2 \tan\varphi\, \Delta s_1$$

$$= \Delta s_1 - \Delta\theta_1 \Delta s_2 (\sec\varphi - \frac{R}{S}\tan\varphi),$$

where the sign of $\Delta\theta_2$ has been taken into account. Hence $\frac{\partial}{\partial s_2}(\Delta s_1) = -\Delta\theta_1(\sec\varphi - \frac{R}{S}\tan\varphi)$. Equation (24) shows that $\Delta\theta_1$ is a constant and it can be taken outside the operator on the left hand side of equation (31), and we have finally

$$\left.\begin{aligned} &\frac{\partial R}{\partial s_2} = -(\sec\varphi - \frac{R}{S}\tan\varphi). \\ \text{Similarly}\quad &\\ &\frac{\partial S}{\partial s_1} = -(\sec\varphi - \frac{S}{R}\tan\varphi). \end{aligned}\right\} \qquad (32)$$

These equations give the variation of the radii of curvature along the failure lines. The corresponding equations for a cohesionless heavy soil have been deduced previously by Massau [4]. When $\varphi = 0$ equations (32) become

$$\frac{\partial R}{\partial s_2} = -1, \qquad \frac{\partial S}{\partial s_1} = -1.$$

and this is an analytical statement of Hencky's second theorem for a Prandtl-Reuss material.

The substitution of $R\Delta\theta_1$ and $-S\Delta\theta_2$ for the arc-lengths Δs_1 and Δs_2 gives an alternative form of equations (32),

$$\left.\begin{aligned} &dS + (R\sec\varphi - S\tan\varphi)d\theta = 0 \quad \text{along a first failure line,} \\ &dR - (S\sec\varphi - R\tan\varphi)d\theta = 0 \quad \text{along a second failure line.} \end{aligned}\right\} \qquad (33)$$

On a first failure line $d\theta = d\alpha$ and $d\theta = \beta$ on a second failure line so that equations (10) can be written

$$\left.\begin{aligned} \frac{\partial v_1}{\partial \alpha} - (v_1 \tan\varphi + v_2 \sec\varphi) = 0, \\ \frac{\partial v_2}{\partial \beta} + (v_2 \tan\varphi + v_1 \sec\varphi) = 0. \end{aligned}\right\}$$

An alternative form of these equations is

$$\left.\begin{aligned} \frac{\partial}{\partial \alpha}[v_1 \exp\{(\beta-\alpha)\tan\varphi\}] - \sec\varphi\, v_2 \exp\{(\beta-\alpha)\tan\varphi\} = 0, \\ \frac{\partial}{\partial \beta}[v_2 \exp\{(\beta-\alpha)\tan\varphi\}] + \sec\varphi\, v_1 \exp\{(\beta-\alpha)\tan\varphi\} = 0. \end{aligned}\right\} \quad (34)$$

In the same way, equations (27) and (28) can be replaced by

$$\left.\begin{aligned} \frac{\partial}{\partial \alpha}[\bar{y} \exp\{(\beta-\alpha)\tan\varphi\}] + \sec\varphi\, \bar{x} \exp\{(\beta-\alpha)\tan\varphi\} = 0, \\ \frac{\partial}{\partial \beta}[\bar{x} \exp\{(\beta-\alpha)\tan\varphi\}] - \sec\varphi\, \bar{y} \exp\{(\beta-\alpha)\tan\varphi\} = 0, \end{aligned}\right\} \quad (35)$$

and equations (33) become

$$\left.\begin{aligned} \frac{\partial}{\partial \alpha}[S \exp\{(\beta-\alpha)\tan\varphi\}] + \sec\varphi\, R \exp\{(\beta-\alpha)\tan\varphi\} = 0, \\ \frac{\partial}{\partial \beta}[R \exp\{(\beta-\alpha)\tan\varphi\}] - \sec\varphi\, S \exp\{(\beta-\alpha)\tan\varphi\} = 0. \end{aligned}\right\} \quad (36)$$

With equations (23), the exponential term in equations (34), (35), (36) can be written

$$\exp\{(\beta-\alpha)\tan\varphi\} = \exp\left\{\tfrac{1}{2}\log\frac{p}{p_0}\right\} = \left(\frac{p}{p_0}\right)^{\frac{1}{2}}.$$

It can easily be deduced from equations (34), (35), (36) that each of the quantities v_1, v_2, $\bar{x}$, $\bar{y}$, R, S multiplied by $\exp\{(\beta-\alpha)\tan\varphi\}$ satisfies the differential equation

$$\frac{\partial^2 f}{\partial\alpha\partial\beta} + \sec^2\varphi\, f = 0. \qquad (37)$$

The method of solution of this equation, which is one form of the equation of telegraphy, depends upon the manner in which the boundary conditions on the function f are prescribed. The analytic solution for one type of boundary condition is given below. The solutions for other types follow closely the analytic solutions for the corresponding problems in a Prandtl-Reuss material [10].

We suppose that the stress components are given along a curve Σ which is not a failure line. If only the normal and tangential stresses are given on Σ, two values for the interior stress component can be obtained from the yield condition and the correct value must be determined from the conditions of the problem in question. The stresses on Σ define the variation of p and Θ along Σ, and, from the theory of characteristics, these boundary values define the stress field in the region DEC enclosed by Σ and the two failure lines, one from each family, passing through the end points D,E of Σ and meeting at a point C. In Fig. 10a, the failure line DC is taken to belong to the first family of failure lines. The values of α and β along Σ can be obtained from equations (25) and Fig. 10b shows the configuration in the $\alpha\beta$ plane.

The values of R and S along Σ are obtained as follows. If s is the arc-length along Σ from the point D then

$$\frac{\partial}{\partial s} = \cos(\psi-\varphi)\sec\varphi\, \frac{\partial}{\partial s_1} + \sin\psi\, \sec\varphi\, \frac{\partial}{\partial s_2}, \qquad (38)$$

where ψ is the angle between the first failure direction and the tangent to Σ. Hence, from equation (29),

$$\frac{\partial\theta}{\partial s} = \cos(\psi-\varphi)\ \sec\varphi/R - \sin\psi\ \sec\varphi/S\ ,$$

and also

$$\frac{\partial}{\partial s}[\tfrac{1}{2}\cot\varphi\ \log p] = -\cos(\psi-\varphi)\ \sec\varphi/R - \sin\psi\ \sec\varphi/S$$

from equations (5) and (29). R and S are therefore given at points on Σ by the relations

$$\left.\begin{aligned}\frac{1}{R} &= \frac{-\cos\varphi}{2\cos(\psi-\varphi)}\frac{\partial}{\partial s}[\tfrac{1}{2}\cot\varphi\ \log p - \theta],\\ \frac{1}{S} &= -\frac{\cos\varphi}{2\sin\psi}\frac{\partial}{\partial s}[\tfrac{1}{2}\cot\varphi\ \log p + \theta].\end{aligned}\right\} \qquad (39)$$

The derivatives of R and S with respect to β and α respectively are known along Σ from equations (36) when R and S are known along Σ. The other derivatives can then be calculated from the equation

$$\frac{\partial f}{\partial s} = \left\{\cos(\psi-\varphi)\sec\varphi/R\right\}\frac{\partial f}{\partial\alpha} - \left\{\sin\psi\ \sec\varphi/S\right\}\frac{\partial f}{\partial\beta}\ , \qquad (40)$$

which follows from equation (38) and the definitions of R, S.

The boundary values of $(\bar{x}, \bar{y})$ are given immediately by equations (26) so that the boundary values of the quantities $\bar{x}\exp\{(\beta-\alpha)\tan\varphi\}$, $\bar{y}\exp\{(\beta-\alpha)\tan\varphi\}$ can be found. The derivatives of these quantities at points on Σ are calculable from equations (35) and (40).

We suppose also that v_1 and v_2 are specified on the curve Σ. The boundary values assigned to v_1, v_2 must be compatible with the stress boundary conditions on Σ in order

to ensure that the resulting velocity solution has non-negative dilatation everywhere. The quantities $v_1 \exp\{(\beta-\alpha)\tan\varphi\}$, $v_2 \exp\{(\beta-\alpha)\tan\varphi\}$ are then known on Σ and the derivatives of these quantities at points on Σ can be found from equations (34) and (40). This is equivalent to specifying a member of the pair (v_1, v_2) and one of its derivatives since the other member of the pair can be determined from equations (34) and (40).

Thus the problem of determining the quantities (v_1, v_2), $(\bar{x}, \bar{y})$ and (R, S) in the region DEC is reduced to the problem of determining a function $f(\alpha, \beta)$ which satisfies equation (37) and which has prescribed values for f and one of its derivatives on the curve Σ. The other derivatives at points on Σ can be obtained from equation (40). Let $P(a,b)$ be a point in the region DEC and let AP and BP be the failure lines through P meeting the curve Σ at A and B. Employing the method of Riemann, a particular solution of equation (37) with certain properties to be defined later will be denoted by $G(\alpha, \beta)$. It follows that the expression

$$\left(G \frac{\partial f}{\partial \alpha} - f \frac{\partial G}{\partial \alpha}\right) d\alpha + \left(f \frac{\partial G}{\partial \beta} - G \frac{\partial f}{\partial \beta}\right) d\beta \qquad (41)$$

is a perfect differential since

$$G \frac{\partial^2 f}{\partial \alpha \partial \beta} = -Gf \sec^2 \varphi = f \frac{\partial^2 G}{\partial \alpha \partial \beta} .$$

The integral of the expression (41) taken around any closed curve is therefore zero and if the expression is integrated around the curve APBA there results

$$0 = \int_A^P \left(f \frac{\partial G}{\partial \beta} - G \frac{\partial f}{\partial \beta}\right) d\beta + \int_P^B \left(G \frac{\partial f}{\partial \alpha} - f \frac{\partial G}{\partial \alpha}\right) d\alpha$$

$$+ \int_B^A \left\{\left(G \frac{\partial f}{\partial \alpha} - f \frac{\partial G}{\partial \alpha}\right) d\alpha + \left(f \frac{\partial G}{\partial \beta} - G \frac{\partial f}{\partial \beta}\right) d\beta\right\}. \qquad (42)$$

In order to evaluate the first two integrals explicitly, the function $G(\alpha, \beta)$ is now defined to be such that $G = 1$ on AP and BP. This implies that $\frac{\partial G}{\partial \beta} = 0$ on AP and $\frac{\partial G}{\partial \alpha} = 0$ on BP and, after some re-arrangement, equation (39) gives

$$f_P = \tfrac{1}{2}(f_A + f_B) + \tfrac{1}{2} \int_B^A \left\{\left(G \frac{\partial f}{\partial \alpha} - f \frac{\partial G}{\partial \alpha}\right) d\alpha + \left(f \frac{\partial G}{\partial \beta} - G \frac{\partial f}{\partial \beta}\right) d\beta\right\}. \qquad (43)$$

It can be shown that the particular function G is given by

$$G(\alpha, \beta) = J_0[2 \sec \varphi \{(a-\alpha)(b-\beta)\}^{\frac{1}{2}}],$$

where $J_0(\xi)$ is the Bessel function of order zero,

$$J_0'' + \frac{J_0'}{\xi} + J_0 = 0, \qquad J_0(0) = 1, \qquad J_0'(0) = 0.$$

Equation (43) therefore expresses the value of f at the point P in terms of f and its derivatives along AB. f can be replaced by any one of the quantities v_1, v_2, $\bar{x}$, $\bar{y}$, R, S multiplied by $\exp\{(\beta - \alpha) \tan \varphi\}$.

BIBLIOGRAPHY

[1] K. Terzaghi, "Theoretical Soil Mechanics", John Wiley and Sons, p. 22, 1943.

[2] R. T. Shield, "Mixed Boundary Value Problems in Soil Mechanics", Q. Appl. Math., 11, No. 1 (1953).

[3] V. V. Sokolovsky, "Statics of Earthy Media", Izdatelsvo Akademii Nauk S. S. R., Moscow, 1942.

[4] J. Massau, "Mémoire sur l'intégration graphique des équations aux derivées partielles", Edition du Centenaire, Comité National de Mécanique, Bruxelles, pp. 121-391, 1952 (reprinted from Ann. de l'Ass. des Ing. sortis des Ecoles spec. de Gand, 1900-1904).

[5] F. Kötter, "Die Bestimmung des Drucks an gekruemmten Gleitflaechen, eine Aufgabe aus der Lehre vom Erddruck", Berlin Akad. Berichte, 229-233 (1903).

[6] D. C. Drucker and W. Prager, "Soil Mechanics and Plastic Analysis or Limit Design", Q. Appl. Math., 10, pp. 157-165 (1952).

[7] R. von Mises, "Mechanik der plastischen Formaenderung von Kristallen", Z. angew. Math. Mech. 8, 161-185 (1928).

[8] W. Prager, "Discontinuous Solutions in the Theory of Plasticity" Courant Anniv. Vol., pp. 289-299, 1948.

[9] E. H. Lee, "On Stress Discontinuities in Plane Plastic Flow", Proc. 3rd Symposium on Appl. Math., McGraw-Hill Book Co., pp. 213-228, 1950.

[10] R. Hill, "The Mathematical Theory of Plasticity", Oxford Univ. Press, 1950.

[11] L. Prandtl, "Ueber die Eindringungsfestigkeit (Haerte) plastischer Baustoffe und die Festigkeit von Schneiden", Z. angew. Math. Mech. 1, 15-20 (1921).

[12] A. Winzer and G. F. Carrier, "The Interaction of Discontinuity Surfaces in Plastic Fields of Stress", J. Appl. Mech. 15, 261-264 (1948).

[13] H. Hencky, "Ueber einige statisch bestimmte Faelle des Gleichgewichts in plastischen Koerpern", Z. angew. Math. Mech. 3, 241-251 (1923).

[14] S. Christianovich, "The Plane Problem of the Mathematical Theory of Plasticity in the Case Where the External Forces are Applied along a Closed Contour", Mat. Sbornik, 1, pp. 511-534 (1936).

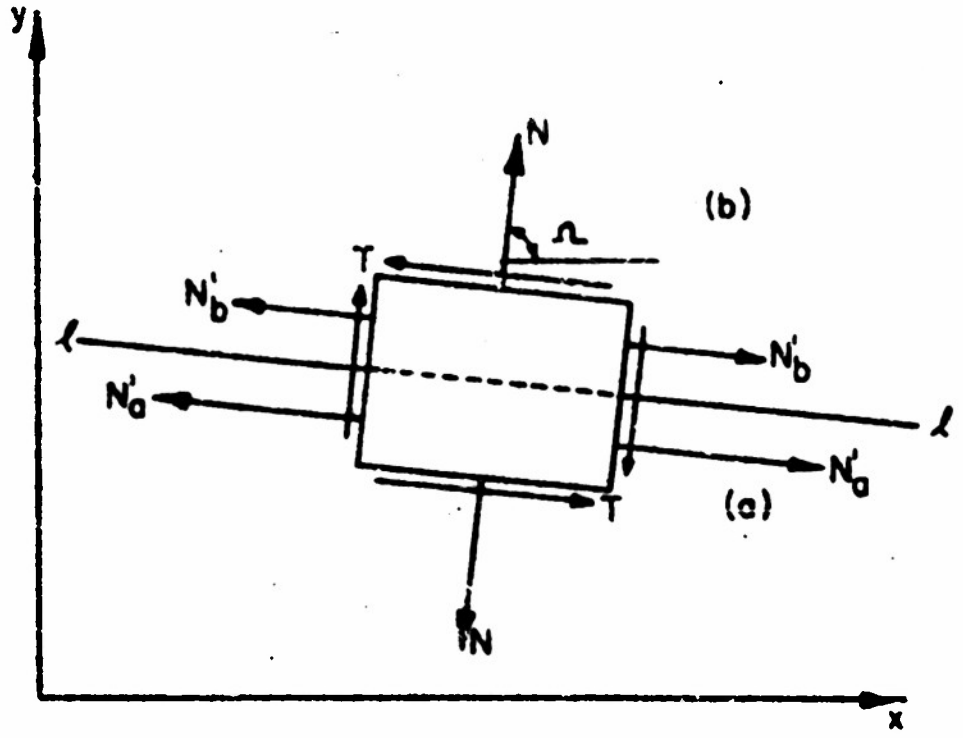

FIG. 1. STRESS DISCONTINUITY

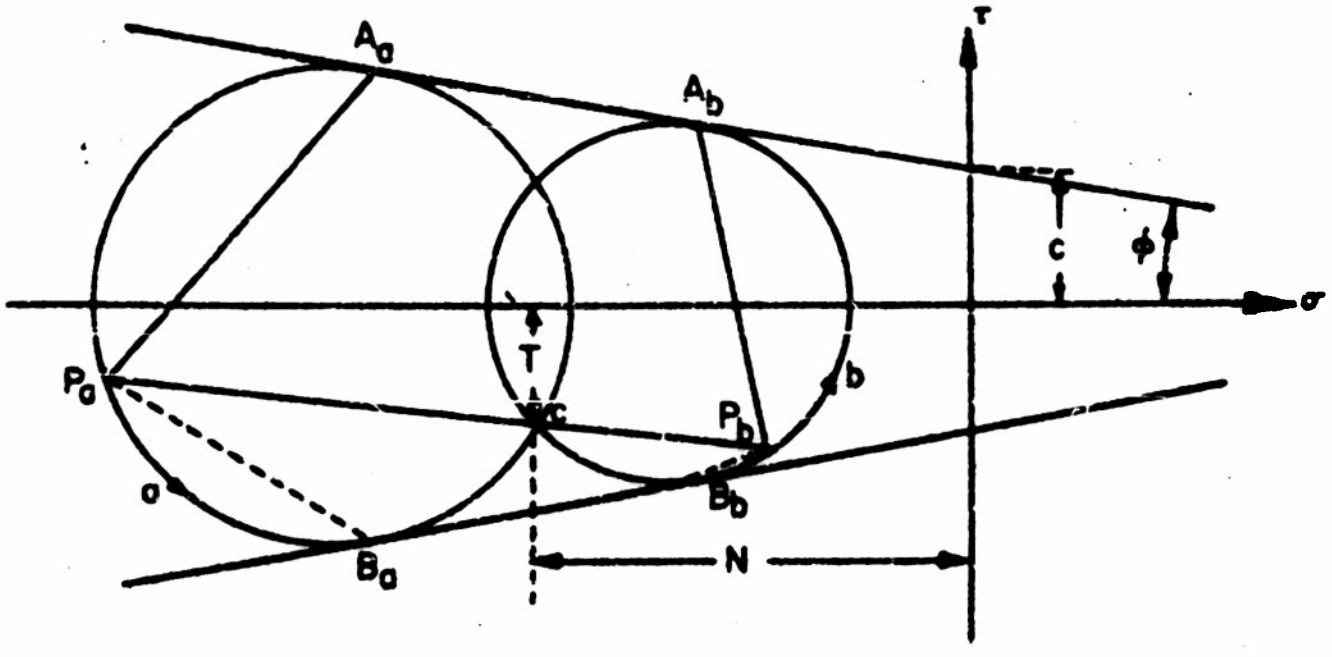

FIG. 2. MOHR'S CIRCLES FOR FIG. 1

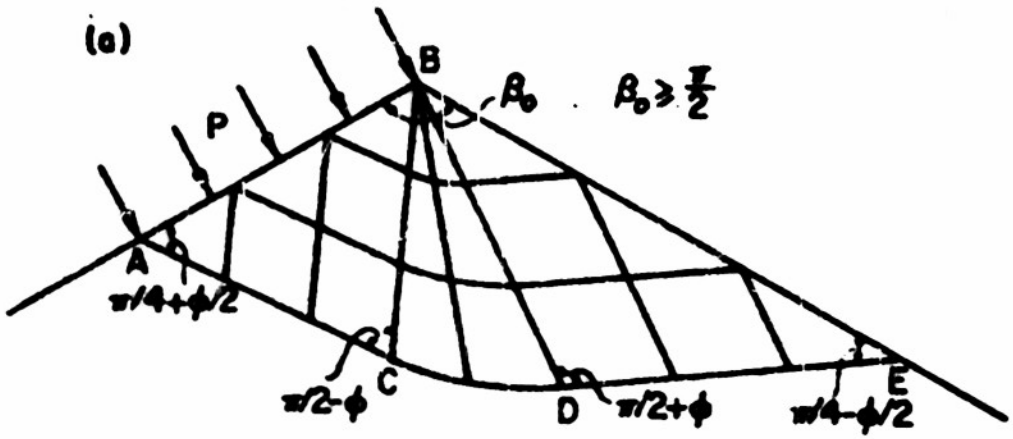

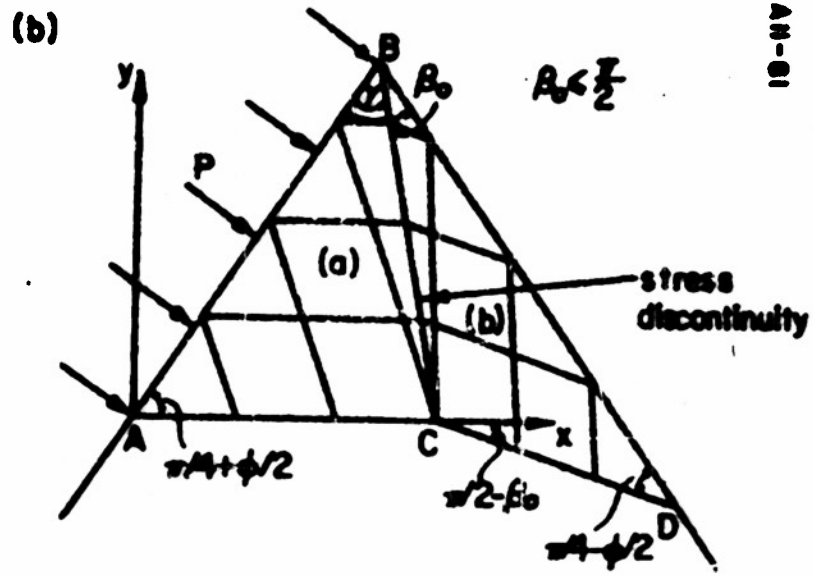

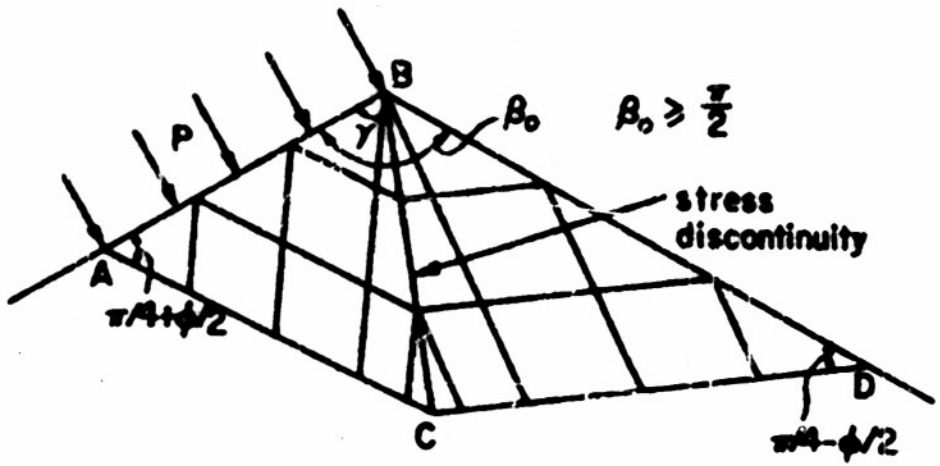

FIG. 3. STRESS FIELDS FOR LOADED WEDGE

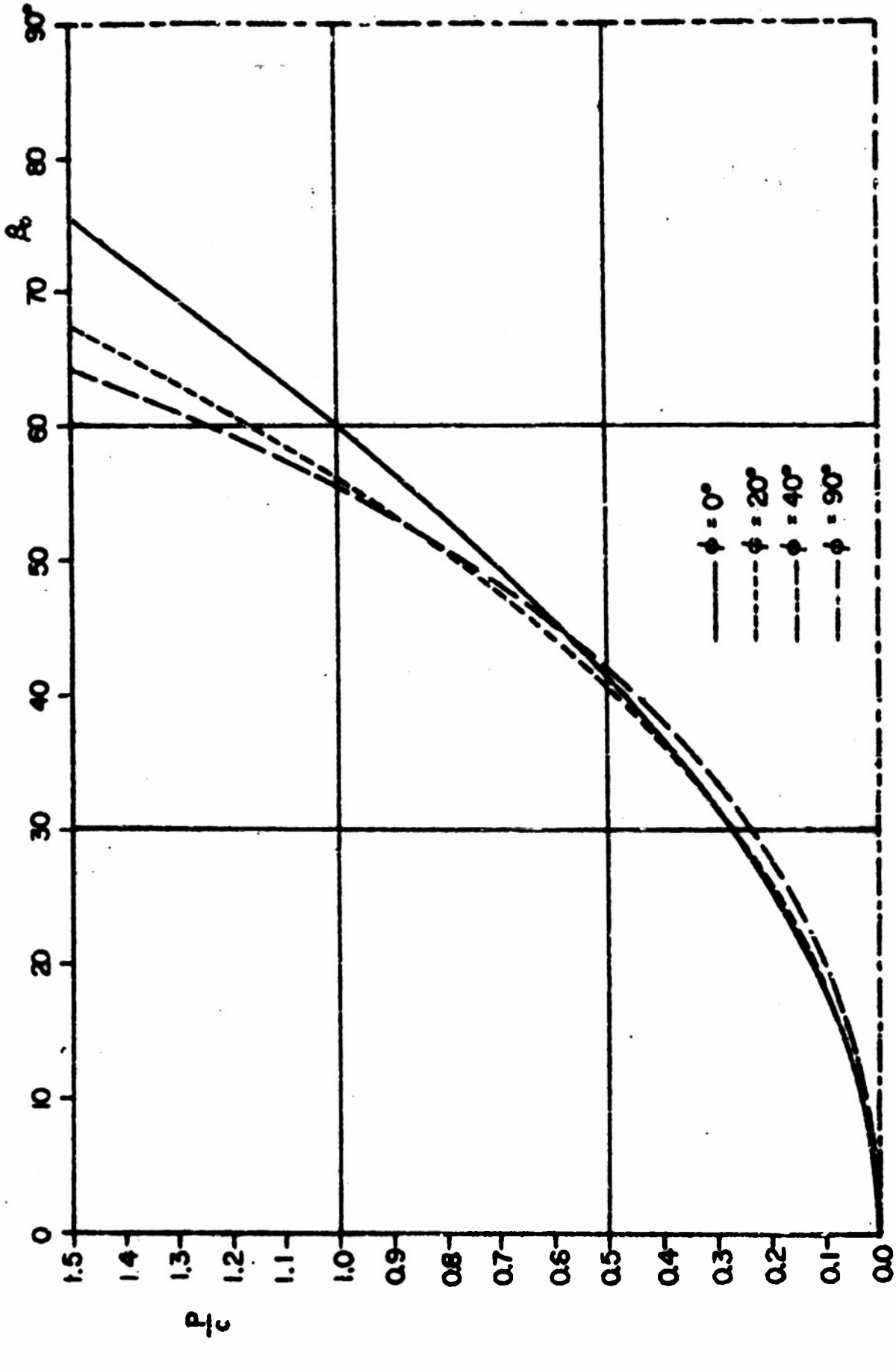

FIG. 4a. PRESSURE ON FACE OF ACUTE ANGLED WEDGE

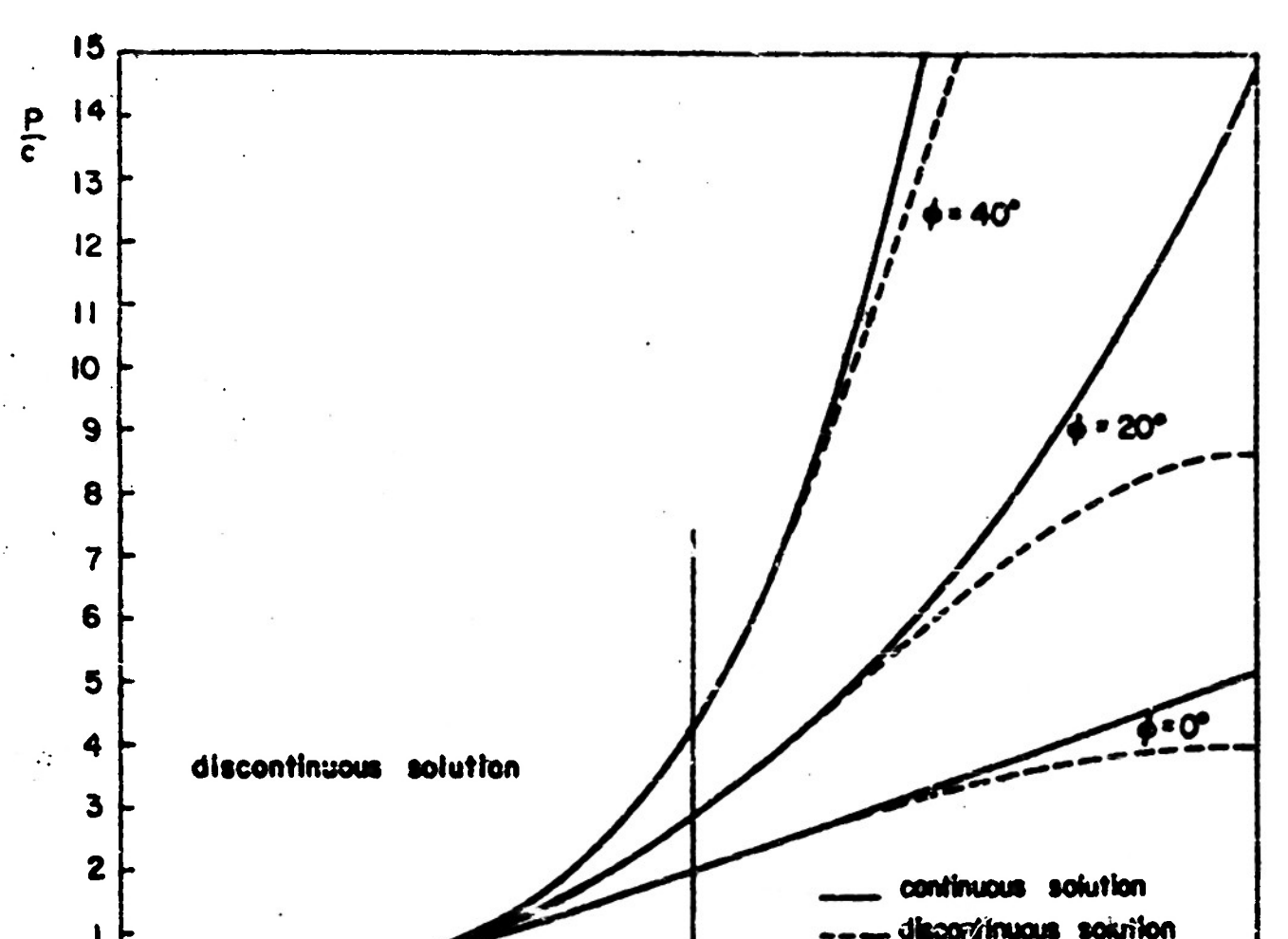

FIG. 4b. PRESSURE ON WEDGE FACE AS GIVEN BY THE DISCONTINUOUS AND CONTINUOUS SOLUTIONS

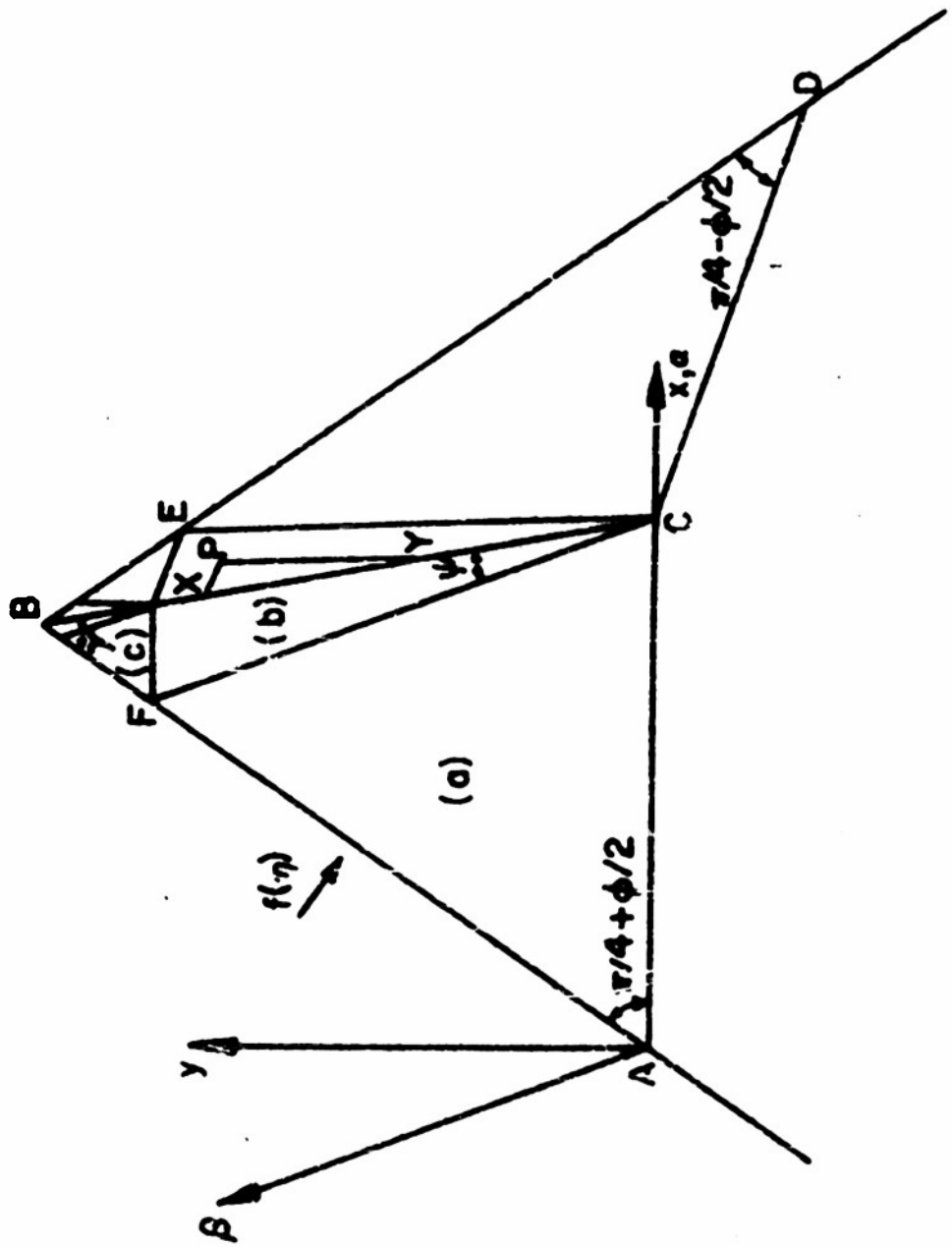

FIG. 5. FAILURE LINE PATTERN FOR ACUTE WEDGE

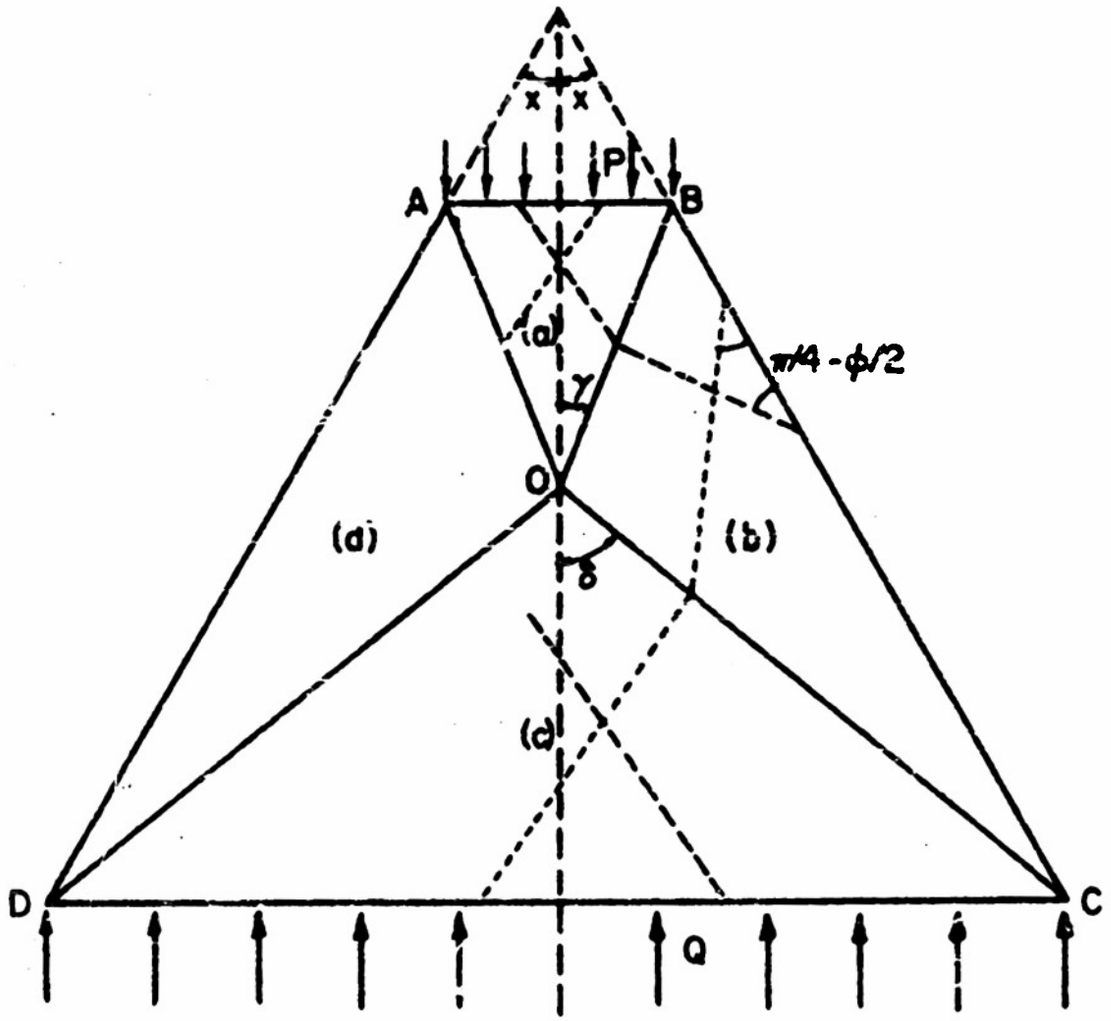

FIG. 6a. DISCONTINUOUS STRESS SYSTEM FOR LOADED TRAPEZOID

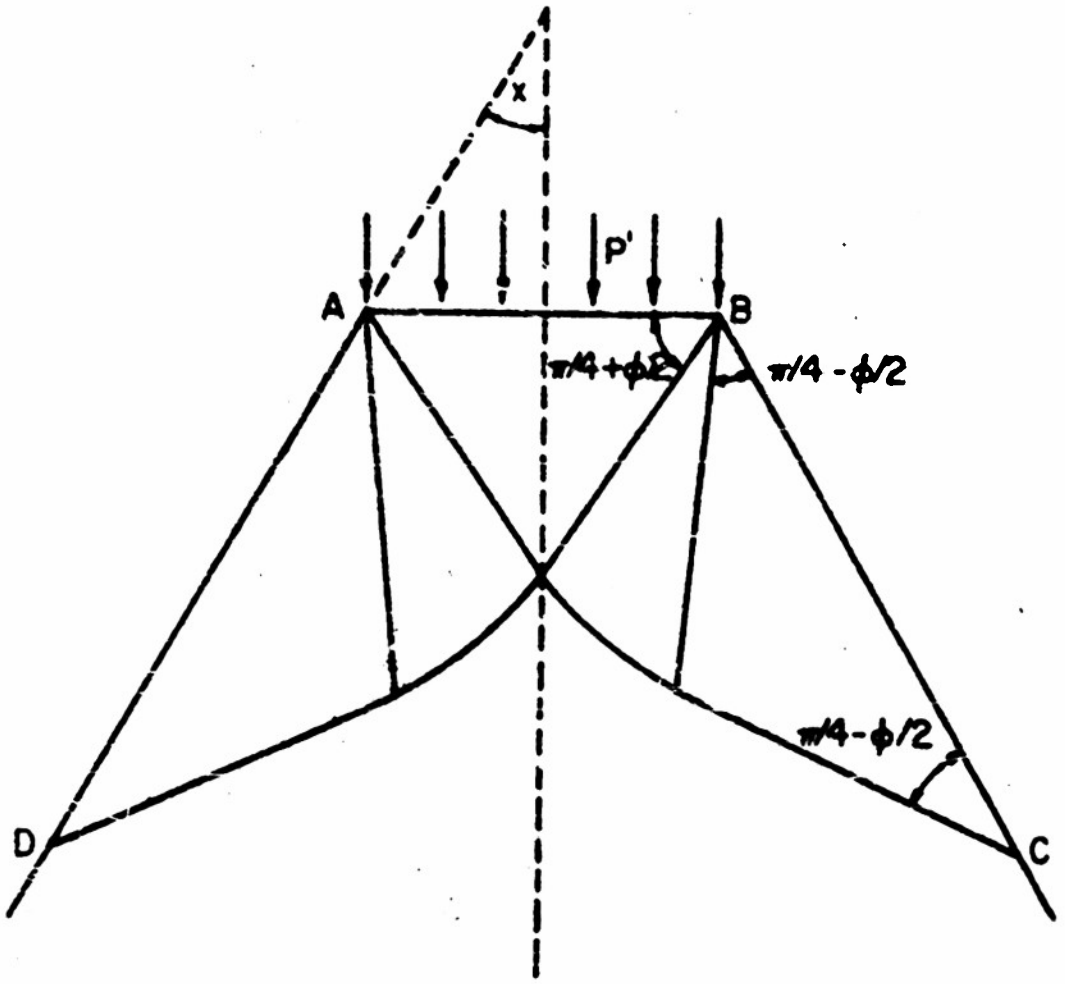

FIG. 6b. CONTINUOUS STRESS FIELD FOR TRUNCATED WEDGE

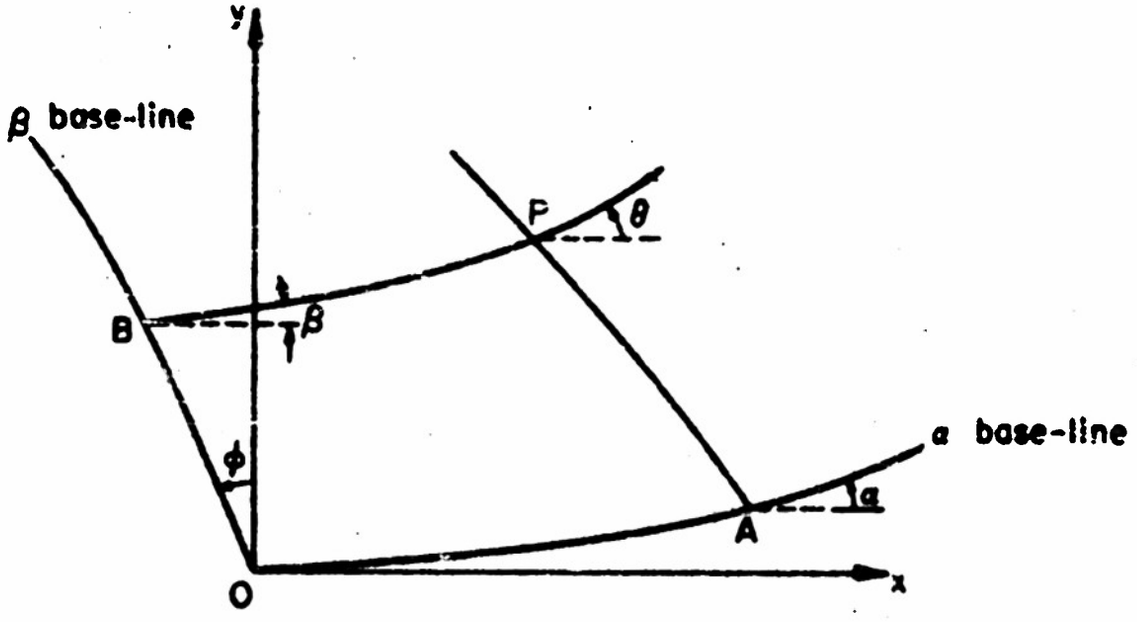

FIG. 7. DEFINITION OF THE CURVILINEAR COORDINATES α, β

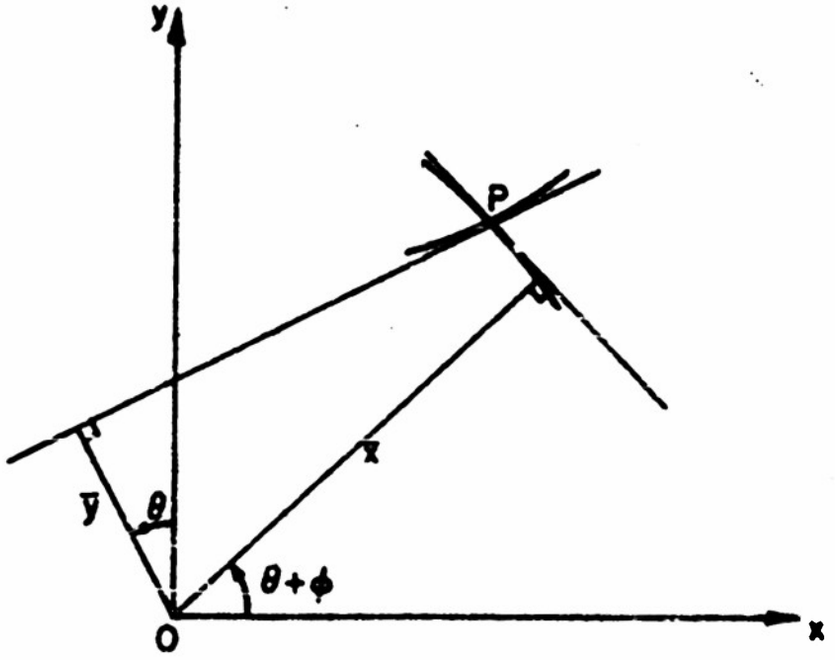

FIG. 8. GEOMETRICAL SIGNIFICANCE OF THE QUANTITIES $\bar{x}, \bar{y}$

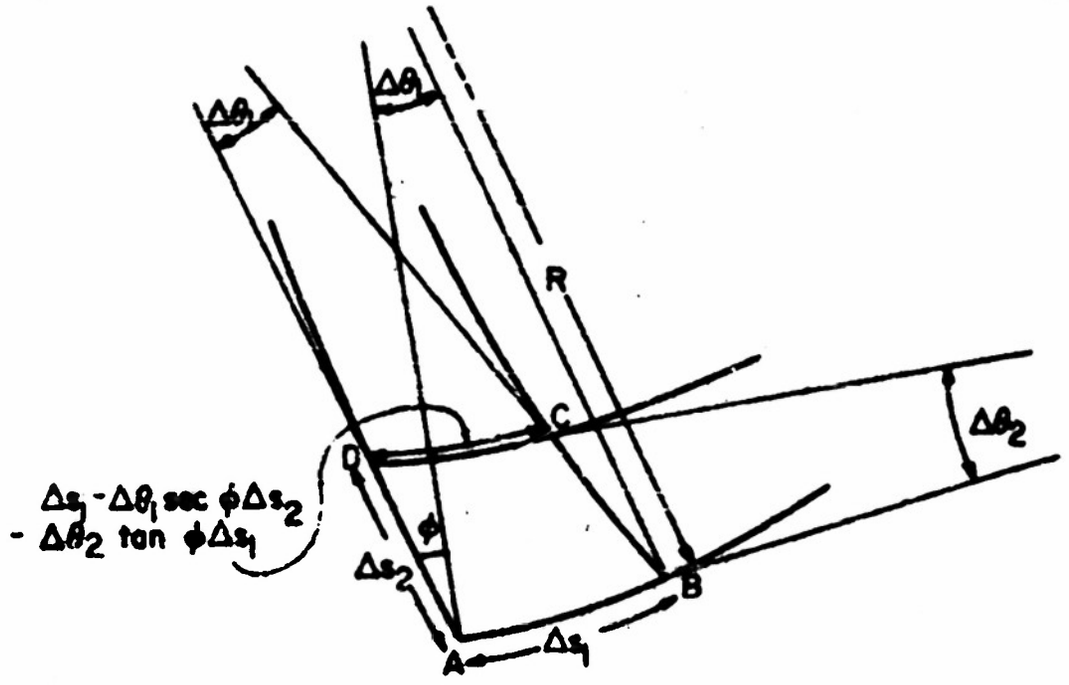

FIG. 9. CURVILINEAR PARALLELOGRAM FORMED BY NEIGHBORING FAILURE LINES

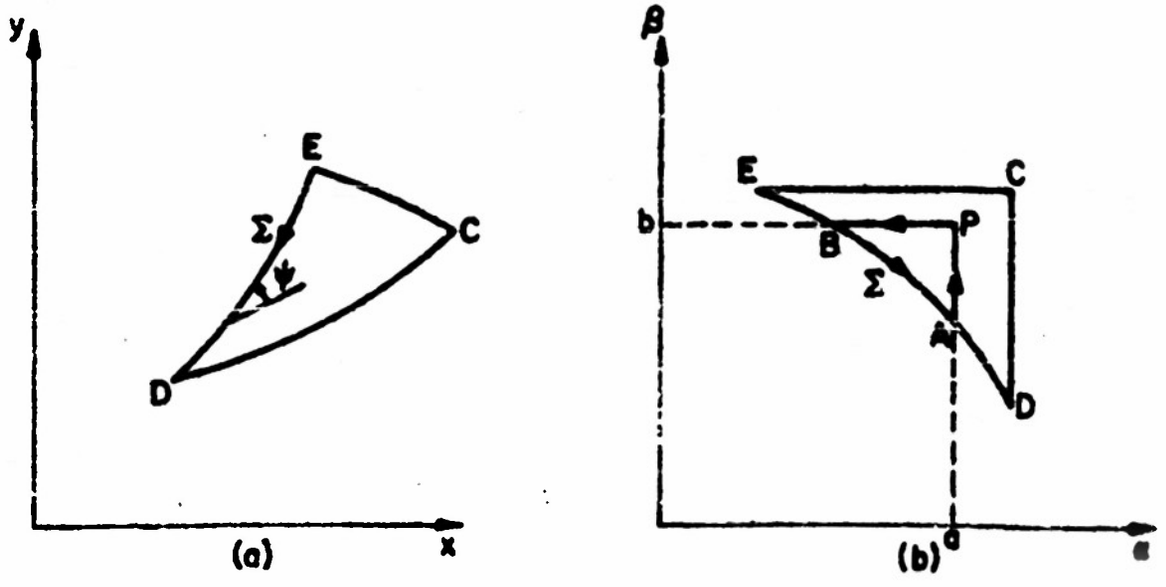

FIG. 10. FAILURE LINES AND BOUNDARY CURVE Σ IN BOUNDARY VALUE PROBLEM CONSIDERED